Submitted to IEE
SQE →
1887

Double-Clad Structures and Proximity Coupling for Diode-Bar-Pumped Planar Waveguide Lasers

C.L.Bonner, T.Bhutta, D.P.Shepherd*, and A.C.Tropper

Optoelectronics Research Centre

University of Southampton

Highfield, Southampton SO17 1BJ, U.K.

email dps@orc.soton.ac.uk

Abstract

We report, for the first time, fabrication of double-clad planar waveguide structures and their use for multi-Watt, diode-bar-pumped, planar waveguide lasers based on Nd^{3+}- and Yb^{3+}-doped YAG. The direct-bonded, five-layer structures of Sapphire, YAG and rare-earth-doped YAG have sufficient numerical aperture to capture the fast-axis divergence of a diode-bar by proximity coupling with no intervening optics, leading to very simple and compact devices. The restriction of the doped region to the central core leads to diffraction-limited laser output in the guided direction. We also show that the direct-bonding fabrication process can lead to a linearly polarised output.

I. INTRODUCTION

Laser media with high-aspect-ratio, slab geometries are known to have improved thermal limitations in comparison to cylindrical rods [1]. This makes them attractive for high power laser systems where the accompanying large thermal load can cause optical distortions and even fracture. Planar thin-film waveguides can be seen as an extreme case of the slab geometry with typical aspect ratios of ~1000 to 1. The planar geometry is also well-suited to high-power diode-array pumping, either by in-plane pumping with diode bars [2],[3] or by face pumping with diode stacks [4]. In bulk materials, high-power diode pumping has been achieved via reflective pumping chambers [5], fibre-coupling [6], lens-ducts [7], and beam-shaping systems [8]. For fibre lasers, double-clad geometries [9] and novel v-groove designs [10] have also been employed. However, the basic geometrical compatibility between planar waveguides and high-power diode arrays can lead to significant simplification of the diode coupling scheme and hence to very compact laser systems. The ease of access to the guided wave in planar thin films also allows the possibility of integrating various functions, such as switching, grating reflectors and filters, polarisation control etc., in a monolithic device.

For planar waveguides, face pumping has the advantage of scalability through the area of the pumped face but suffers due to the very low single-pass pump absorption through the thin doped core layer, requiring relatively thick, and hence multi-guided-mode, waveguides and the use of a reflective pumping chamber [4]. In-plane coupling is certainly more restricted in power, as pumping is limited to a small number of diode-bars, but it still has the potential for allowing pumping levels of >100W. The advantages of the in-plane pumping scheme include a much stronger single-pass pump absorption and compatibility with very small waveguide dimensions (<10μm) leading to high optical gains per unit pump power.

It has recently been shown that directly-bonded, rare-earth-doped YAG on Sapphire waveguides are well-suited to in-plane pumping by diode bars [11]. Their high numerical aperture (0.46) allows efficient coupling via fibre/rod lenses for guides with cores as small as 4μm, despite the non-diffraction-limited nature of the fibre-lens-collimated diode pump beam. This leads to a compact overall device and output powers approaching 4W have been obtained from a Nd:YAG/Sapphire waveguide when pumped with a 20W diode bar. However, the output

of these devices is non-diffraction-limited due both to the multimode nature of the structure in the guided plane and to the high Fresnel number of the monolithic cavity in the non-guided plane. Here we demonstrate diode-bar-pumped waveguide lasers that are diffraction-limited in the guided plane by the use of a double-clad, multi-layer, planar waveguide structure. Such structures have previously been employed in high-power fibre lasers [12] and consist of a single-mode, rare-earth-doped, lasing core surrounded by a much larger inner-cladding that captures the diode pump beam. The pump light is gradually absorbed each time it passes through the doped region, and single-spatial-mode laser output is obtained. For planar guides the size of the core, relative to the inner-cladding, is much larger in order to avoid increasing the effective absorption length for the pump light beyond the practical limitations of planar fabrication. We describe how this can lead to a new regime of operation for double-clad structures where the selection of the output spatial mode is controlled by the confinement of the doping rather than the optical confinement of the core. Hence the device works by gain mode selection rather than by cladding-pumping of a single mode core. We also show that such structures can readily be pumped by simply proximity coupling the diode-bar, leading to even more compact devices ($<1 cm^2$ footprint) with no need for coupling optics.

Following the introduction this paper is organised as follows. Section II discusses the design and fabrication of the 5-layer planar double-clad structures, the advantages and limitations of the high core-to-cladding size ratio regime, and how related designs are also being pursued in fibre and bulk lasers. In section III a double-clad Yb:YAG waveguide is characterised by Ti:Sapphire end-pumping, demonstrating the low propagation loss, high gain, and linearly polarised, diffraction-limited output mode quality of this structure. In section IV we describe the experimental set-up for proximity coupling of diode-bars to planar guides and discuss the results obtained for coupling into an 8μm core-thickness Nd:YAG on Sapphire waveguide. In section V we discuss the results obtained for proximity-coupled, side-pumped Nd^{3+}- and Yb^{3+}-doped YAG, double-clad waveguide structures, demonstrating multi-Watt, single-guided mode outputs in both cases. Finally, in section VI, we give our concluding remarks and discuss the possibilities for also controlling the mode in the non-guided plane in order to obtain fully diffraction-limited devices.

II. DESIGN AND FABRICATION OF DOUBLE-CLAD PLANAR WAVEGUIDES

Fig. 1(a) shows a typical double-clad guiding structure for high-power fibre lasers and amplifiers. The single-mode core is surrounded by a considerably larger, multi-mode, inner cladding. This, in turn is surrounded by an outer cladding which has a much lower refractive index. In this way the non-diffraction-limited diode pump beam can be contained in the high-numerical aperture (NA) waveguide made by the two claddings. The doped core gradually absorbs the pump radiation each time it bounces through it, leading to a much longer effective absorption length compared to bulk glass of the same doping level. Indeed, various design tricks, such an off-centre core or a non-circular inner cladding, are often used to help absorb helical pump modes which otherwise could avoid passing through the doped region at all. For a fibre, the increased length required, often to lengths of several tens of metres, is not a significant problem in terms of fabrication or increased loss. However, most planar fabrication techniques are rather limited in the length of device that can be produced and the associated propagation losses are more severe. This leads to the typical design shown in fig.1(b), where the low NA, single-mode, doped core is a significant fraction of the overall pumped region. This leads to an increased absorption efficiency, in both a bouncing ray model and in terms of overlap of the doped region with the guided pump modes. The rather small pumping dimension is not a problem for the planar geometry because we have no requirement to circularise the diode-beam and we can take advantage of its near-diffraction-limited nature in the fast axis. The drawback to this design is the possibility of a significant overlap of the higher-order modes of the inner-cladding waveguide with the gain region, increasing the possibility of a non-diffraction-limited output.

The waveguides used in our experiments were fabricated by Onyx Optics Inc. by the direct-bonding method [11],[13]. This technique allows precision-polished materials to be joined together by Van der Waals intermolecular forces, with bond strengths sufficient to withstand further polishing down to layer thicknesses of a few microns. This allows the production of multi-layer waveguides with bulk optical properties and low propagation losses. Fig. 2(a) shows the dimensions and refractive index profiles for the double-clad waveguides used in the following laser experiments. The outer cladding is made of sapphire oriented with the (001) direction parallel to the plane of the waveguide core and in the direction of propagation for the laser output. This material is very durable, polishes well, and has a high thermal conductivity. The

inner cladding is made of undoped YAG, which again has good mechanical and thermal properties and is known to bond well to sapphire [11]. This outer guidance structure has a NA of ~0.46 which is sufficient to optically confine the highly-divergent output from a typical diode bar, when proximity coupled to the waveguide. The core consists of rare-earth-doped YAG, which is the standard high-power solid-state laser material. Guidance in the core region can arise from the increase in refractive index associated with the rare-earth doping. Table 1 gives the relevant index values used for our design which were taken from the following references [14],[15],[16],[17]. The values used for the increase in index due to the doping are based on measurements taken at 633nm, but it is has been observed that this index difference does not change dramatically with wavelength [16], and so should still be valid out to 1.1μm.

Fig. 2(b) shows the predicted propagation modes (in this case TE modes) at the laser wavelength for the core waveguide, assuming an infinite inner cladding layer thickness. It can be seen that both waveguides allow two propagation modes and in both cases the fundamental mode has nearly, but not fully, decayed by the time it reaches the outer cladding layer. Fig. 2(c) shows predicted TE modes at the laser wavelengths for the inner cladding guide assuming no core and an infinite outer cladding layer. In both cases the fundamental mode and the highest-order mode are shown (the Nd^{3+}-doped structure support 28 modes and the Yb^{3+}- doped structure supports 18). It can clearly be seen that the higher-order modes of the cladding guide have a substantial overlap with the gain region and if the guide was doped throughout the cladding guide we would expect a multi-mode laser output. However, the fundamental mode has the best overlap with the confined doped region, and the smallest mode size, and so should reach laser threshold first. Due to the confinement of the doped region the fundamental mode can saturate all the available gain, stopping the higher-order modes from reaching threshold, and hence a single-mode output is obtained. The fundamental mode in question should be that of the overall 5-layer structure, rather than those shown in figure 2, because the core modes still have a noticeable mode-intensity at the boundary with the outer cladding layer. A question then arises as to whether the index change associated with the doping is of any importance at all. Fig. 3 shows a comparison of the fundamental modes of the 5-layer structures (a) with and (b) without this small index rise. It can clearly be seen that the index rise leads to a stronger confinement of the mode to the doped region. This will lower its threshold but could make it harder for it to saturate the gain fully. A brief summary of the theory used to calculate the mode profiles

described in this section is given in appendix 1.

Thus we can see that this is a new operating regime for double-clad lasers that is not strictly the same as that described as cladding-pumping where the core size is much smaller than the inner cladding and the lasing mode is truly associated with the core guiding structure. This new regime could perhaps be more accurately described as gain mode selection, and it begins when the mode of the core starts to have appreciable intensity at the boundary with the outer cladding region. Clearly, if the core to cladding size ratio is pushed to near to 1 the higher order modes will start to see unsaturated gain and could start to lase, but we will experimentally demonstrate in section V that ratios of 0.67 for Nd:YAG and 0.44 for Yb:YAG give single-mode laser outputs. The advantage of such high ratios is the increased absorption efficiency. As we have already stated this is of particular relevance to planar devices, but large mode areas can also be of interest in high-power pulsed fibre lasers in order increase energy storage capabilities. This has already inspired work on large mode area fibres [18] where the fundamental mode of a multimode core is selected by only doping the central region. A cladding-pumped version of this fibre design has also recently been reported [19], but in this case the mode selection is still strictly from amongst those associated with the core rather than the overall structure. However it is possible that the desire for further increases in power could push double-clad fibre lasers into the high core to cladding ratio regime. It is also interesting to note that a core-doped bulk laser, also made by direct bonding, has recently been demonstrated which shows enhanced beam-quality over a uniformly-doped rod [20]. In this case mode selection occurs between those allowed by the optical resonator rather than those allowed by a multi-mode waveguide.

III. Ti-SAPPHIRE PUMPED DOUBLE CLAD Yb:YAG WAVEGUIDE LASER

In order to characterise the novel double-clad structures in terms of propagation loss, gain, polarisation behaviour, and mode quality, the end-pumped laser performance of the Yb^{3+}-doped guide described in section II was assessed using a Ti:Sapphire pump laser. The 5mm by 10mm guide had its end-faces polished plane and parallel. An estimate of the absorption length for 10at.% Yb^{3+}-doped YAG was made from the results of Lacovara et al [21], giving values of ~1.1mm at 941nm and 968nm, and ~1.9mm at 915nm. For the Ti:Sapphire pumping we chose to use the weaker absorption at 915nm due to the pump laser having a greater output power at

this wavelength. A rough estimate of the absorption length for the double-clad guide was made by increasing this figure according to the ratio of the undoped to doped areas of the pumped region. Thus we expected an absorption length of 4.3mm, which allowed us to choose to pump the waveguide along the 5mm-long direction. The laser resonator was formed by the end-faces of the waveguide with the addition of butted plane mirrors as required.

Initially, using a X6 microscope objective, we took care to couple the pump light into the waveguide such that propagation of a fundamental pump mode was observed by imaging the output onto a CCD camera. The 1.029μm lasing threshold was then determined as a function of the output coupling. The use of only Fresnel reflections (8.4%) or HR mirrors helps to avoid possible etalon effects between the end-faces and the butted mirror causing an effective output coupling different to the normal transmission of the mirror. The fact that lasing occurred off the bare end-faces of the waveguide at a threshold of just 500mW incident power demonstrates the high gain available from the waveguide configuration (in this case a round-trip gain of 21.5dB). Assuming that the laser has the same mode size in each case, and that there is no change in losses with changing pump intensity, the threshold, P_{th}, should obey the following equation,

$$P_{th} = k\left(2\sigma_a N_1 l - \ln(R_1 R_2) + 2\alpha l\right)$$

where k is a constant dependent upon the material parameters, the pump launch efficiency, and the pump and signal spatial properties, σ_a is the absorption cross-section at the laser wavelength, N_1 is the lower laser level population density, l is the length of the cavity, R_1 and R_2 are the mirror reflectivities, and α is the propagation loss coefficient. Therefore a plot of the threshold versus $-\ln(R_1R_2)$ should have an intercept on the $-\ln(R_1R_2)$ axis of $-(2\sigma_a N_1 l + 2\alpha l)$. Such a plot is shown in fig. 4. Using $\sigma_a = 1.8\times10^{-24}$ m^2, $N_1 = 6.9\times10^{25}$ m^{-3} (5% of the total population) and $l = 5\times10^{-3}$ m, we find a value for α of 5m^{-1} or equivalently 0.2dB/cm. Thus this 5-layer waveguide has losses equivalent to those found for previously fabricated 2-layer direct-bonded waveguides, [11],[13].

The focusing of the Ti-Sapphire pump laser was then changed by using a 5cm focal-length lens instead of the X6 objective. When viewed on the CCD camera it was clear that we were now coupling to the higher-order modes of the 5-layer structure, as we would with a high-power diode-laser. Under these conditions the combined launch and absorption efficiency was

calculated to be 0.77 by comparing the measured pump power before and after the guide. Taking into account the rough estimate of the absorption length made above we can estimate that this corresponds to a near 100% launch efficiency, which is not surprising for such a large and high NA waveguide pumped by a Ti:Sapphire laser. The output efficiency and mode quality was tested using a cavity formed by one HR mirror and one bare end-face of the waveguide. The results are shown in figure 5. The high slope efficiency of 76% (59%) with respect to absorbed (incident) power is in-line with what may be expected for Yb (the quantum limit for 915nm pumping is 89%), but it is another indication of the high quality of the double-clad waveguide. The mode profile of the lasing output was investigated using both a CCD camera and a Coherent M^2 meter. No matter how badly we attempted to launch the pump light in order to propagate high-order pumping modes, we were only able to see a single-mode waveguide laser output. The output intensity profile imaged onto the CCD camera is shown in figure 6. The clean single-lobed output is not, in itself, proof of a single-mode, diffraction-limited, behaviour but when M^2 measurements were taken a value of 1.2 was found in the guided direction. In fact, in this case the M^2 value in the non-guided direction was also near 1.0 and so we have a truly diffraction-limited output. However, as will be shown in the later sections, diode-array pumping would lead to a much larger gain region in this non-guided plane and hence to a multi-mode output. The output was at 1.029μm, which is at the peak of the Yb emission spectrum, and was found to be TE polarised. The linearly polarised output is in contrast to the randomly polarised output previously observed with 2-layer YAG on sapphire guides, and is perhaps an indication of increased stress in the 5-layer structures, leading to a difference in TM and TE propagation losses and/or mode sizes that is sufficient to give a polarised laser emission. At present it is not known if such effects are responsible for this behaviour, but in practice this is a very convenient way of obtaining a polarised output which may be useful for future application to non-linear frequency conversion.

IV. PROXIMITY COUPLING

For our first demonstration of proximity coupling we used a waveguide consisting of an 8μm thick Nd:YAG core contact-bonded to a sapphire substrate. The guide was 18mm long by 2mm wide and was end-polished on all four faces to allow lasing along the long axis and pumping

along the short axis. This pumping region is much thinner than would be the case for a double-clad structure and so represents a strong test of the capabilities of the proximity coupling technique. The 807nm Jenoptik diode bar had an output power of 10W and a 1cm by 1μm emission aperture. Fig. 7 shows the experimental apparatus used to achieve proximity coupling. The diode and waveguide are mounted on separate water-cooled heatsinks and these are held on their own manipulators. The diode can easily be brought to within a few tens of microns of the waveguide by observation of their separation with a microscope. They can then be aligned to have the same separation across the length of the diode and, by observing the diffraction pattern, their relative orientations can be corrected such that they are parallel to each other. Observation of the fluorescence intensity allows the relative heights to be adjusted. The diode and waveguide are then moved closer, taking care to make any further small corrections in their orientations, until optimum laser output is achieved. By measuring the pump power before and after the waveguide and accounting for Fresnel reflections, a combined launch and absorption efficiency factor of 0.45 was deduced. Using a bulk piece of Nd:YAG with the same doping level, an absorption length of 3mm was measured for a similar diode. Thus we arrive at a proximity-coupling launch efficiency of nearly 90%. Thus it is clear that this is not only a very simple and compact coupling scheme, but it is also very efficient when used for high-numerical-aperture (0.46) guides, even for sub-10μm core widths. Observation of the fluorescence intensity showed that it gradually increased, with interferometric-like fluctuations, as the diode approached the waveguide and that it became steady when contact was made. However, it was not clear whether this contact was between the waveguide and the diode facet or another part of the surrounding contacts as it was difficult to tell if the facet was slightly recessed or not. Optimum laser performance did not necessarily occur at this contacted point.

The side-pumped laser performance of the guide was quickly tested by butt-coupling an HR and a 77%R mirror to the end-faces of the waveguide. Over 0.5W of laser output was obtained for 6W of incident power but, as would be expected, it was highly multi-mode. Indeed in the non-guided direction it was observed that lasing paths involving reflections off the polished side faces of this long, thin guide were occurring. Nevertheless, our primary aim of demonstrating the feasibility of proximity coupling had been achieved.

VI. PROXIMITY-COUPLED, DIODE BAR SIDE-PUMPED, Nd^{3+}- AND Yb^{3+}-DOPED

YAG. DOUBLE-CLAD WAVEGUIDE LASERS

The 1cm long by 5mm wide, double-clad, Nd^{3+}- and Yb^{3+}-doped guides described in section II were side-pumped by 20W diode-bars, at 807nm and 941nm respectively, using the same proximity coupling set-up as described in section V. Due to the larger overall pumping areas the alignment was found to be easier than for the 8μm core-pumped waveguide described earlier. Fig.8 shows the laser output power versus incident pump power for both lasers. For the Yb-doped sample an upper limit to the combined launch and absorption efficiency factor was measured to be 63% by measuring the pump power before and after the waveguide. This was an upper limit as we were not able to catch all the pump light after the waveguide. We would expect the launch efficiency to be near to 100% and so the 5mm width of double-clad waveguide appears to be approximately one absorption length for the diode pump. The Yb laser results were taken using a 7% output coupler and show a 14.5% slope efficiency with respect to incident power, and hence (also accounting for one Fresnel reflection) a slope efficiency of ≥23% with respect to absorbed power. With optimisation at the high pump level a maximum output power of 2.2W was obtained, but attempts to increase the output power by using a mirror to reflect any left over pump light back into the waveguide were unsuccessful. The output wavelength in this case was found to be around 1048nm, corresponding to the transition to the highest stark level of the $^4F_{7/2}$ ground level. While this transition has a much lower emission cross-section than the 1029nm line it also suffers less from ground state-absorption and so can quite easily be made to lase[22]. The output was found to be TE polarised as had previously been observed with Ti:Sapphire pumping. The far-field output profile of the beam in the guided direction was measured by scanning the vertical intensity profile of one section of the output. Figure 9 shows that the results fit well to a Gaussian profile, and that measuring the second moment radius at various distances from the guide gives a divergence of 64.1mrad. The calculated radius of the fundamental mode of the Yb:YAG double-clad guide is 5.26μm which would lead to an output divergence of 63.4mrad, suggesting that the output is indeed in the fundamental mode and has an M^2 value very close to 1. The output mode is still highly multi-mode, although single-lobed, in the non-guided plane. This is as we expect due to the large gain area and, as yet, no attempt has been made to control the mode in this direction.

Fig.8 also shows the output performance of the Nd:YAG double-clad structure using a

60% reflectivity output coupler. It can be seen that this laser has a lower threshold (~5W) and a higher slope efficiency with respect to incident power (~20%) than the Yb:YAG laser. With optimisation at the maximum pump power an output power of ~4W was obtained. Once again the output divergence is consistent with a fundamental guided-mode output. In this case the output is at 1.064μm and was found to be TE polarised.

VII. CONCLUSIONS

We have demonstrated the first double-clad planar waveguide lasers based on Nd^{3+}- and Yb^{3+}-doped YAG. These structures give a single guided-mode multi-Watt output when pumped by high-power diode-bars. The desire to keep the device to maximum dimensions of ~1cm has led to a high core-to-cladding size ratio and mode selection occuring due to the confinement of the gain rather than the cladding-pumping of a single-mode core, as is normally the case in fibre lasers. We have also shown that such structures are well-suited to proximity-coupled diode pumping, which leads to very compact devices where the diode and waveguide footprint is $<1cm^2$. Work in the immediate future will concentrate on obtaining outputs that are also diffraction-limited in the non-guided plane. Here the problem is to couple the broad gain area to a single spatial mode without compromising the simple monolithic nature of our current devices. Routes to this end could include 2-dimesional double-clad structures, unstable resonators, and adiabatic tapers. The introduction of passive Q-switching sections is also of great interest for the near future. It is our aim to develop such technologies and combine them with the highly-compact and simple devices produced to date.

ACKNOWLEDGEMENTS

The authors would like to acknowledge Raymond J. Beach and Helmuth E. Meissner for useful discussions. The Optoelectronics Research Centre is an EPSRC (UK) interdisciplinary research centre.

APPENDIX 1

The following section describes the modelling of the propagation modes of a 5-layer symmetric waveguide. Fig.10 shows the modelled structure. It is to be expected that symmetric (even) and asymmetric (odd) field solutions will exist due to the symmetry of the structure. The mode effective indices will lie between n_1 and n_3 and so we would expect exponential decay in region 3, oscillatory behaviour in region 1, and both in region 2 (as the effective index can be greater or smaller than n_2). With this in mind we choose the TE field solutions below,

$$E_y = \begin{pmatrix} A_3 e^{-\alpha_3 x} & \text{region 3} \\ A_2 e^{-\alpha_2 x} + A_2' e^{\alpha_2 x} & \text{region 2} \\ A_1 \begin{bmatrix} \cos(k_1 x) \\ \sin(k_1 x) \end{bmatrix} & \text{region 1} \\ \pm\left(A_2 e^{\alpha_2 x} + A_2' e^{-\alpha_2 x}\right) & \text{region 2}' \\ \pm A_3 e^{\alpha_3 x} & \text{region 3}' \end{pmatrix} e^{-ik_z z}$$

where the upper and lower solutions correspond to the even and odd modes. Dispersion relations for the mode constants k_z, k_1, α_2, and α_3 can be obtained by applying the wave equation in the five regions, and the relative field amplitudes, A_n, can be found by applying the boundary conditions of continuity to the electric and magnetic fields [23]. In this way we arrive at the field expressions,

$$E_y = \begin{cases} \left(\frac{2\alpha_2}{\alpha_2+\alpha_3}\right) e^{-d_2(\alpha_2-\alpha_3)} e^{-\alpha_3 x} & \textit{region 3} \\ e^{-\alpha_2 x} + \left(\frac{\alpha_2-\alpha_3}{\alpha_2+\alpha_3}\right) e^{-2d_2\alpha_2} e^{\alpha_2 x} & \textit{region 2} \\ \left[e^{-\alpha_2 d_1} + \left(\frac{\alpha_2-\alpha_3}{\alpha_2+\alpha_3}\right) e^{-\alpha_2(2d_2-d_1)}\right] \begin{bmatrix}\cos(k_1 x)/\cos(k_1 d_1) \\ \sin(k_1 x)/\sin(k_1 d_1)\end{bmatrix} e^{-ik_z z} & \textit{region 1} \\ \pm\left(e^{\alpha_2 x} + \left(\frac{\alpha_2-\alpha_3}{\alpha_2+\alpha_3}\right) e^{-2d_2\alpha_2} e^{-\alpha_2 x}\right) & \textit{region 2}' \\ \pm\frac{2\alpha_2}{\alpha_2+\alpha_3} e^{-d_2(\alpha_2-\alpha_3)} e^{\alpha_3 x} & \textit{region 3}' \end{cases}$$

and the guidance conditions,

$$\begin{bmatrix}\tan \\ \cot\end{bmatrix}(k_1 d_1) = \pm\frac{\alpha_2}{k_1}\left(\frac{\alpha_3+\alpha_2\tanh[\alpha_2(d_2-d_1)]}{\alpha_2+\alpha_3\tanh[\alpha_2(d_2-d_1)]}\right)$$

It can be seen that the guidance condition reduces to the normal three-layer expression [23] by setting $d_1=d_2$.

[1] W. Koechner, *Solid-State Laser Engineering*, 4th ed. (Springer-Verlag, Berlin, 1996) Ch. 7.

[2] U. Griebner, H. Schönnagel, R. Grunwald, S. Woggon, "Transversely guided pumped Yb:YAG laser," in *Tech. Digest of Conference on Lasers and Electro-Optics*, 1997, pp. 307-308.

[3] C.L. Bonner, C.T.A. Brown, D.P. Shepherd, W. A. Clarkson, A. C. Tropper, and D. C. Hanna, "Diode-bar end-pumped high-power Nd:$Y_3Al_5O_{12}$ planar waveguide laser," *Opt. Lett.*, vol. 23, pp. 942-944, 1998.

[4] A. Faulstich, H.J. Baker, and D.R.Hall, "Face pumping of thin, solid-state slab lasers with laser diodes," *Opt. Lett.*, vol. 21, pp. 594-596, 1996.

[5] *for example*, J.J. Chang, E.P. Dragon, C.A. Ebbers, I.L. Bass, and C.W. Cochran, "An efficient diode-pumped Nd:YAG laser with 451W of CW IR and 182W of pulsed green output," in *OSA TOPS on Advanced Solid-State Lasers*, 1998, pp. 300-304.

[6] *for example*, M. Karszewski, U. Brauch, K. Contag, S. Ergard, A. Giesen, I. Johannsen, C. Stewart, and A. Voss, "100W TEM_{00} operation of Yb:YAG thin disc laser with high efficiency," in *OSA TOPS on Advanced Solid-State Lasers*, 1998, pp. 296-299.

[7] R.J. Beach, "Theory and optimization of lens ducts," *Appl. Opt.*, vol. 35, pp. 2005-2015, 1996.

[8] W.A. Clarkson and D.C. Hanna, "Two-mirror beam-shaping technique for high-power diode bars," *Opt. Lett.*, vol. 21, pp. 375-377, 1996.

[9] E. Snitzer, H. Po, F. Hakimi, R. Tumminelli, B.C. McCollum, "Double-clad, offset core Nd fiber laser," in *Proc. Of Conference on Optical Fiber Communication*, 1988, paper PD5.

[10] M. Hofer, M.E. Fermann, and L. Goldberg, "High-power side-pumped passively mode-locked Er-Yb fibre laser," *IEEE Photon. Technol. Lett.*, vol. 10, pp. 1247-1249, 1998.

[11] D.P. Shepherd, C.L. Bonner, C.T.A. Brown, W.A. Clarkson, A.C. Tropper, D.C. Hanna, and H.E. Meissner, "High-numerical-aperture, contact-bonded, planar waveguides for diode-bar-pumped lasers," *Opt. Commun.*, vol. 160, pp. 47-50, 1998.

[12] *for example*, V.Dominic, S.MacCormack, R. Waarts, S. Sanders, S.Bicknese, R. Dohle, E. Wolak, P.S. Yeh, and E. Zucker, "110W fiber laser," in *Tech. Digest of Conference on Lasers and Electro-Optics / Europe*, 1999, post-deadline paper CPD11.

[13] C.T.A. Brown, C.L. Bonner, T.J. Warburton, D.P. Shepherd, A.C. Tropper, D.C. Hanna, and H.E. Meissner, "Thermally bonded waveguide lasers," *Appl. Phys. Lett.*, vol. 71, pp. 1139-1141, 1997.

[14] D.N. Nikogosyan, *Properties of Optical and Laser-Related Materials*, Chichester, UK: Wiley, 1997, p. 5.

[15] D.E. Zelmon, D.L. Small, and R.Page, "Refractive-index measurements of undoped yttrium aluminium garnet from 0.4 to 5.0μm," *Appl. Opt.*, vol. 37, pp. 4933-4935, 1998.

[16] F. Patel, Lawrence Livermore National Laboratory, University of California, "Refractive index measurements of Yb:YAG," *private communication*, 1999.

[17] D. Pelenc, "Guide d'onde laser en Nd:YAG et Yb:YAG per E.P.L.," Ph. D. dissertation, Département Optronique du LETI, C.E.N.G. 85X 38041 Grenoble, France, 1992.

[18] H.L. Offerhaus, N.G. Broderick, D.J. Richardson, R. Sammut, J. Caplen, and L. Dong, "High-energy single-transverse-mode Q-switched fiber laser based on a multimode large-mode-area erbium-doped fiber,"*Opt. Lett.*, vol. 23, pp. 1683-1685, 1998.

[19] H.L. Offerhaus, J.A. Alvarez-Chavez, J. Nilsson, P.W. Turner, W.A. Clarkson, and D.J. Richardson, "Multi-mJ, multi-Watt Q-switched fiber laser," in *Tech. Digest of Conference on Lasers and Electro-Optics*, 1999, post-deadline paper CPD10.

[20] A. Lucianetti, R. Weber, W. Hodel, H.P. Weber, A. Papashvili, V.A. Konyushkin, and T.T. Basiev, "Beam-quality improvement of a passively Q-switched Nd:YAG laser with a core-doped rod," *Appl. Opt.*, vol. 38, pp. 1777-1783, 1999.

[21] P. Lacovara, H.K. Choi, C.A. Wang, R.L. Aggarwal, and T.Y. Fan, "Room-temperature diode-pumped Yb:YAG laser," *Opt. Lett.*, vol. 16, pp. 1089-1091, 1991.

[22] D. Pelenc, B. Chambaz, I. Chartier, B. Ferrand, C. Wyon, D.P. Shepherd, D.C. Hanna, A.C. Large and A.C. Tropper "High slope efficiency and low threshold in a diode-pumped epitaxially-grown Yb:YAG waveguide laser," *Opt. Comm.*, vol. 115, pp. 491-497, 1995.

[23] D.L. Lee, *Electromagnetic Principles of Integrated Optics*, New York, USA: Wiley, 1986, ch.4.

Table 1

Refractive Indices at Pumping and Lasing Wavelengths				
	808nm	941nm	1029nm	1064nm
Sapphire (n_o) [13]	1.760	1.757	1.755	1.755
YAG [14]	1.8212	1.8175	1.8154	1.8147
10at.% Yb:YAG [15]	-	1.8187	1.8166	-
1at.% Nd:YAG [16]	1.8216	-	-	1.8151

Table Captions

Table 1 Refractive indices of the waveguide structure at various wavelengths of interest

Figure Captions

Figure 1 Typical double-clad waveguide designs for high-power diode-pumped lasers and amplifiers in (a) fibre and (b) planar geometries.

Figure 2 The 5-layer refractive index profiles for the double-clad Yb^{3+}- and Nd^{3+}-doped waveguides (a) and theoretical mode profiles for the 3-layer core (b) and cladding (c) waveguides.

Figure 3 The theoretical fundamental mode profiles for the 5-layer structures with (a) and without (b) allowing for the index increase due to the rare-earth doping.

Figure 4 Incident power threshold against $-\ln(R_1R_2)$. The intercept on the x-axis is related to the round trip loss.

Figure 5 Output power against absorbed pump power for the Ti:Sapphire pumped Yb:YAG double-clad waveguide laser.

Figure 6 Imaged single-mode, diffraction-limited output of the Yb:YAG double-clad waveguide laser.

Figure 7 Experimental arrangment for proximity coupling.

Figure 8 Output power versus incident pump power for the double-clad proximity-side-pumped Yb:YAG and Nd:YAG waveguides.

Figure 9 Measured far-field intensity profile for the Yb:YAG waveguide laser in the guided direction with a Gaussian fit. Inset is the measured second moment radius at various distances form the waveguide output.

Figure 10. Symmetric 5-layer waveguide model.

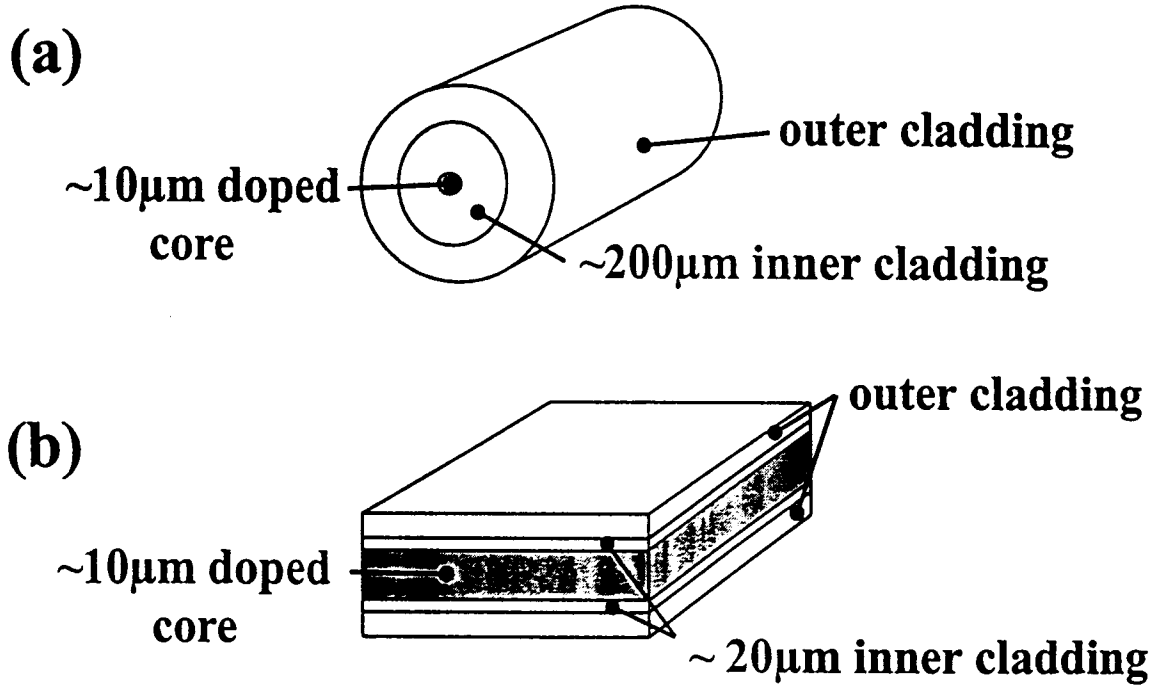
(a)
outer cladding
~10μm doped
core
~200μm inner cladding
(b)
outer cladding
~10μm doped
core
~ 20μm inner cladding

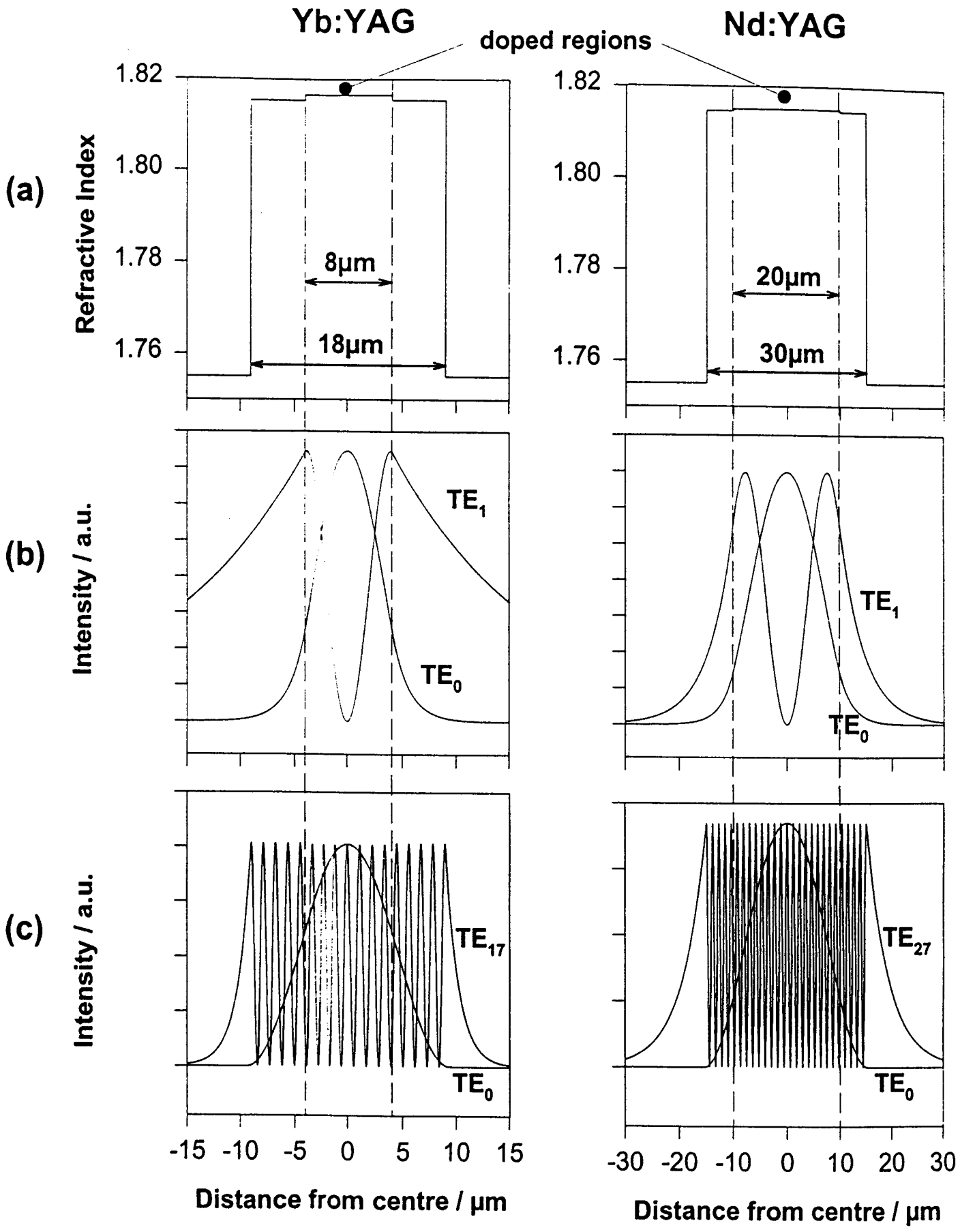
Yb:YAG
Nd:YAG
doped regions
(a)
Refractive Index
1.82
1.80
1.78
1.76
8μm
18μm
20μm
30μm
(b)
Intensity / a.u.
TE1
TE0
(c)
Intensity / a.u.
TE17
TE27
TE0
-15 -10 -5 0 5 10 15
-30 -20 -10 0 10 20 30
Distance from centre / μm
Distance from centre / μm

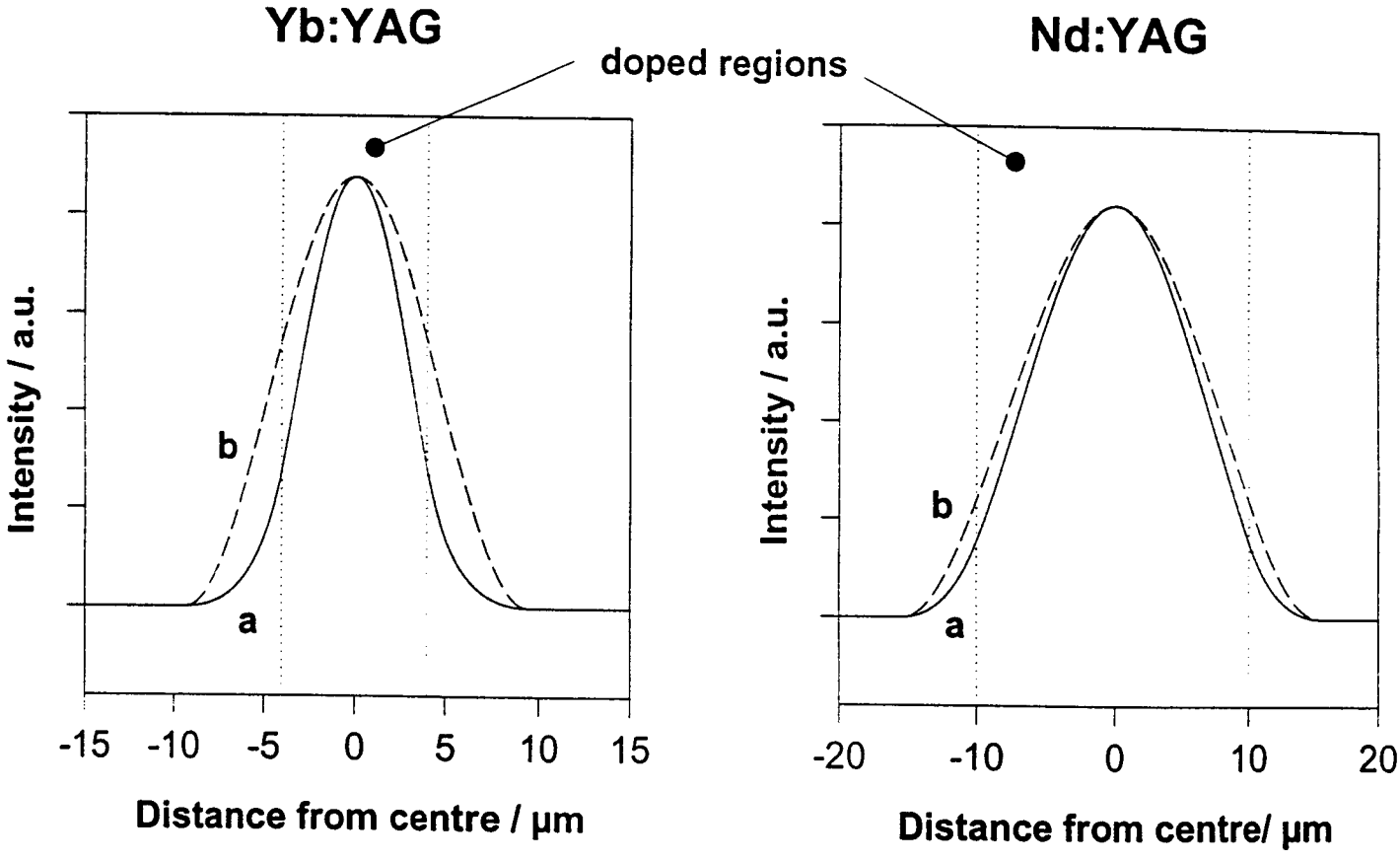
Yb:YAG
doped regions
Nd:YAG
Intensity / a.u.
b
a
-15
-10
-5
0
5
10
15
Distance from centre / µm
Intensity / a.u.
b
a
-20
-10
0
10
20
Distance from centre/ µm

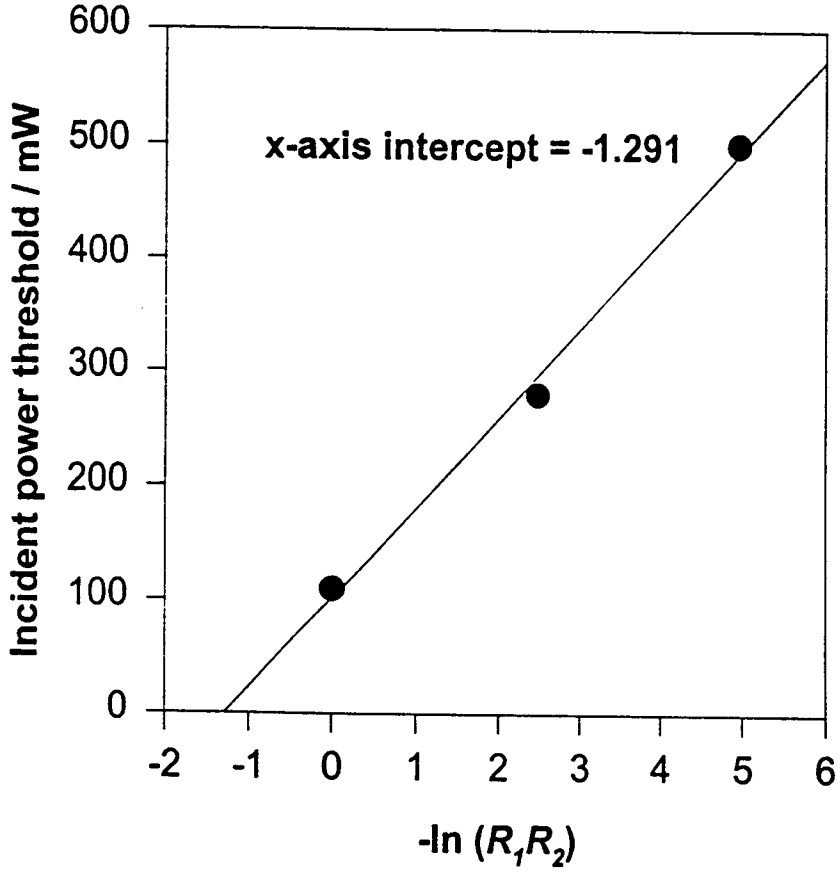
600
500
400
300
200
100
0
Incident power threshold / mW
x-axis intercept = -1.291
-2
-1
0
1
2
3
4
5
6
-ln (R_1R_2)

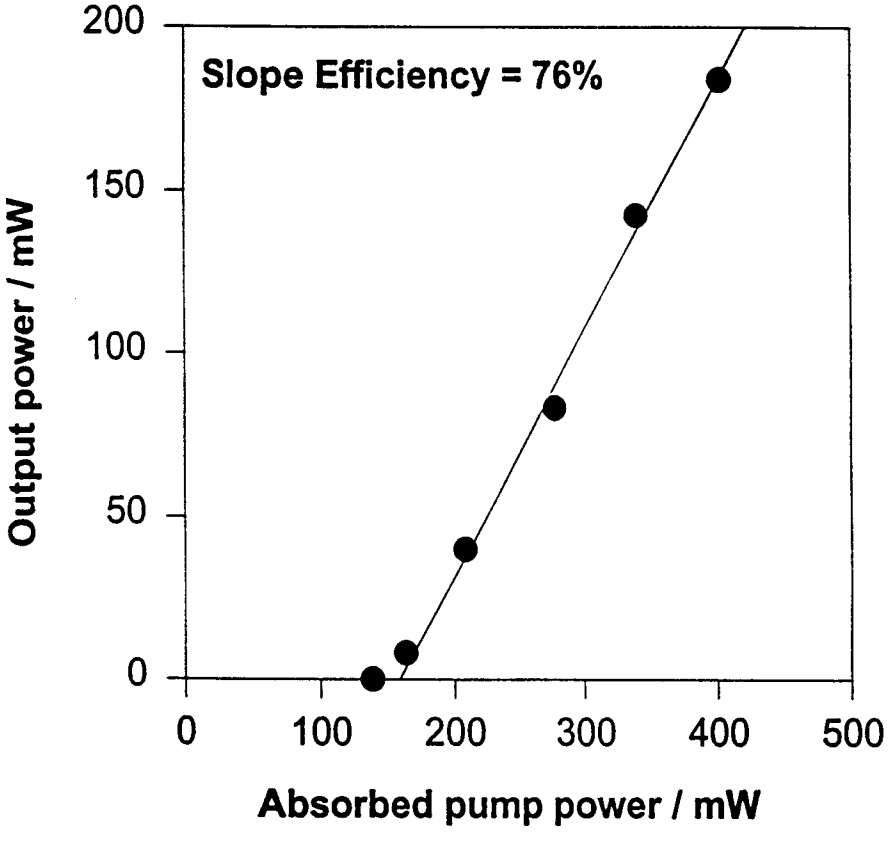
Slope Efficiency = 76%
Output power / mW
Absorbed pump power / mW
200
150
100
50
0
0
100
200
300
400
500

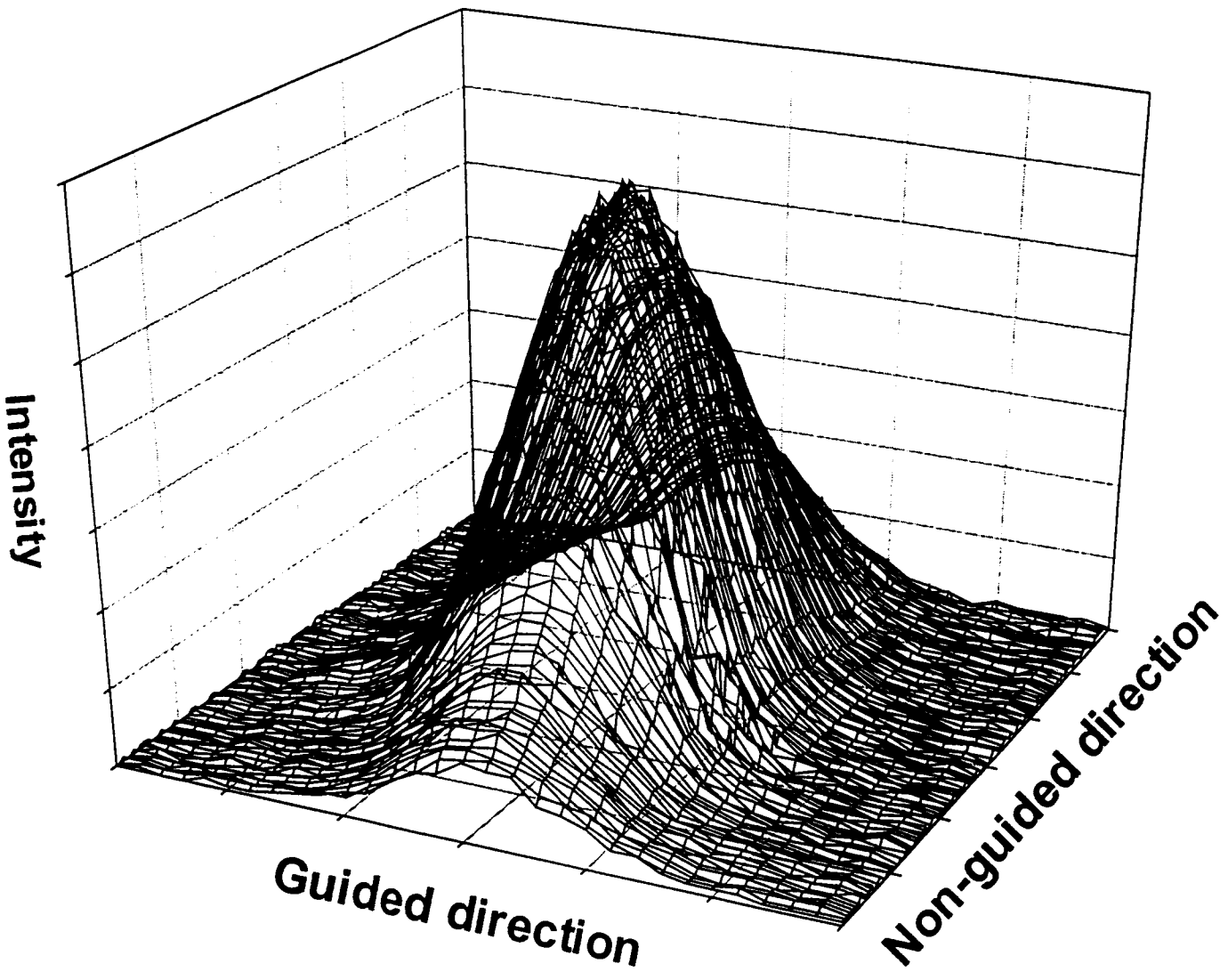
Intensity
Guided direction
Non-guided direction

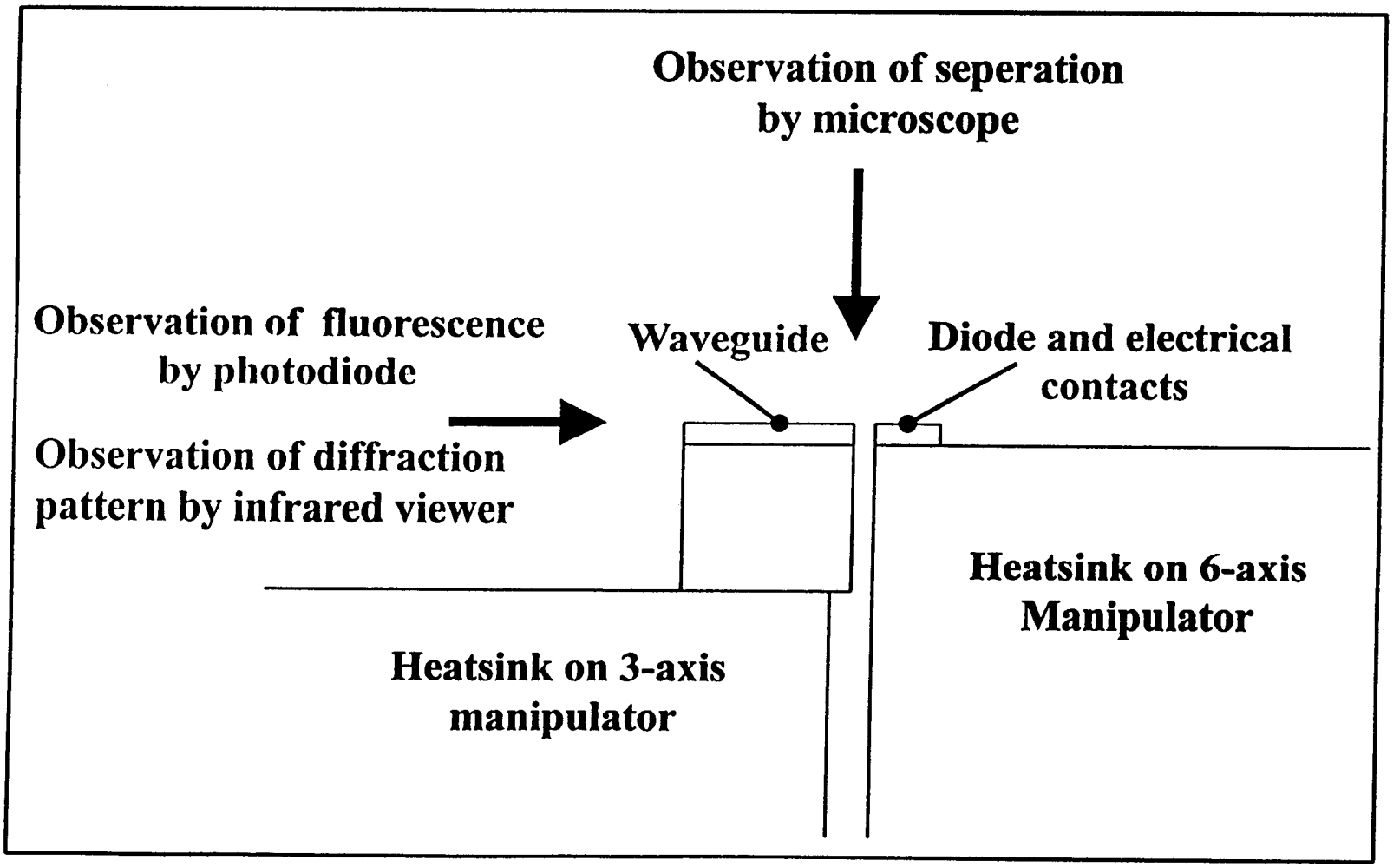
Observation of seperation
by microscope
Observation of fluorescence
by photodiode
Waveguide
Diode and electrical
contacts
Observation of diffraction
pattern by infrared viewer
Heatsink on 6-axis
Manipulator
Heatsink on 3-axis
manipulator

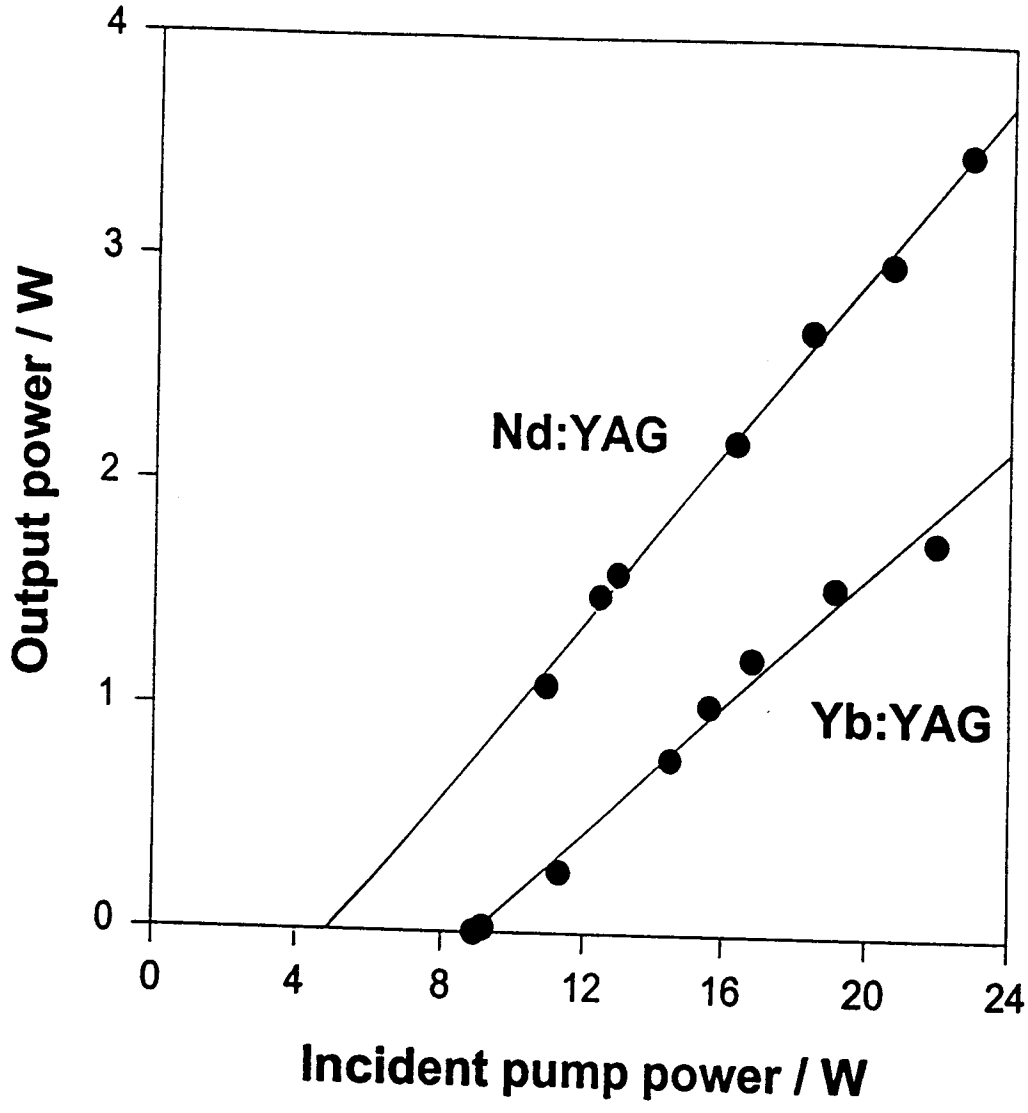
Output power / W
Incident pump power / W
Nd:YAG
Yb:YAG
0
1
2
3
4
0
4
8
12
16
20
24

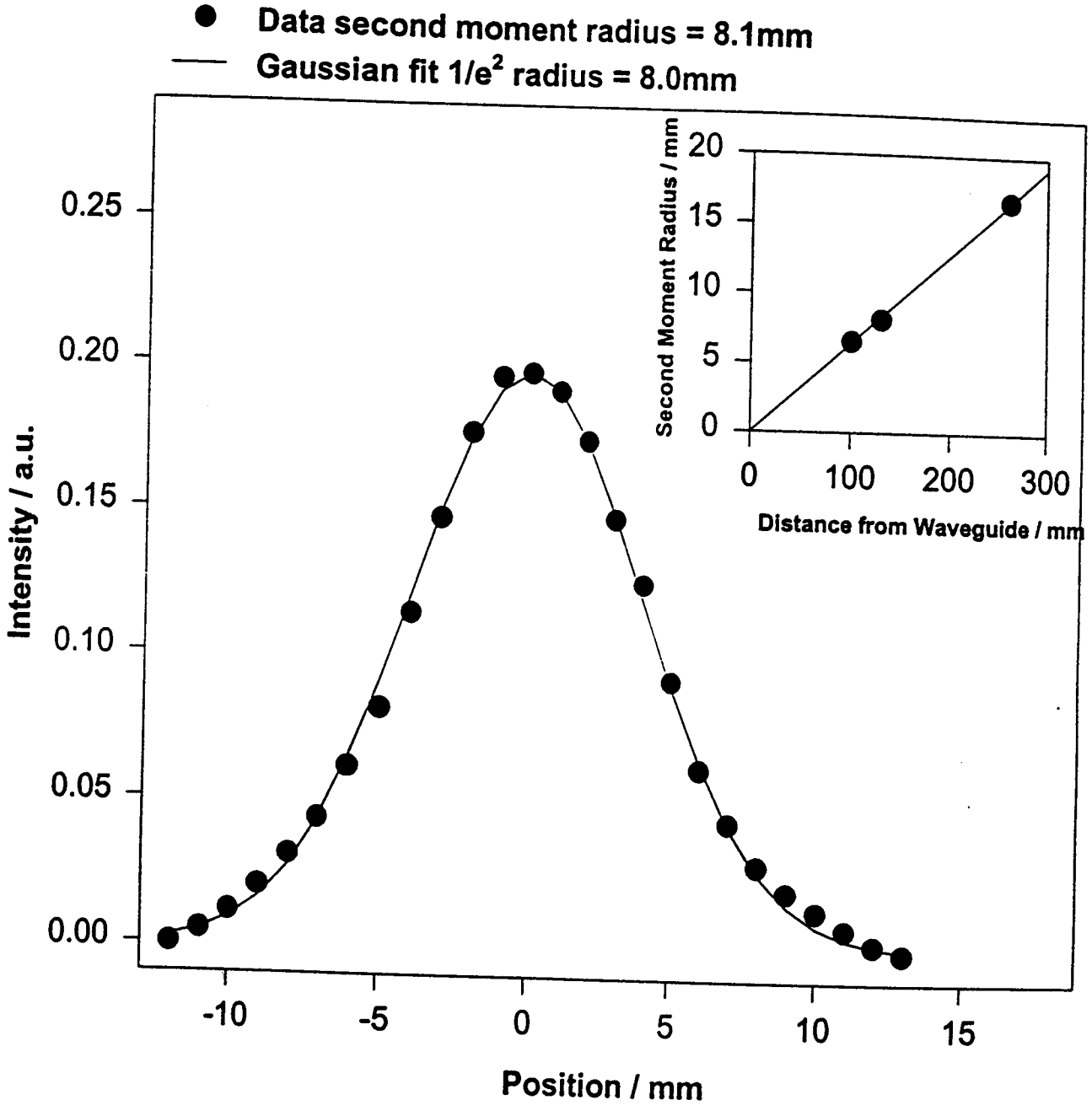
Data second moment radius = 8.1mm
Gaussian fit 1/e² radius = 8.0mm
Intensity / a.u.
0.25
0.20
0.15
0.10
0.05
0.00
-10
-5
0
5
10
15
Position / mm
Second Moment Radius / mm
20
15
10
5
0
0
100
200
300
Distance from Waveguide / mm

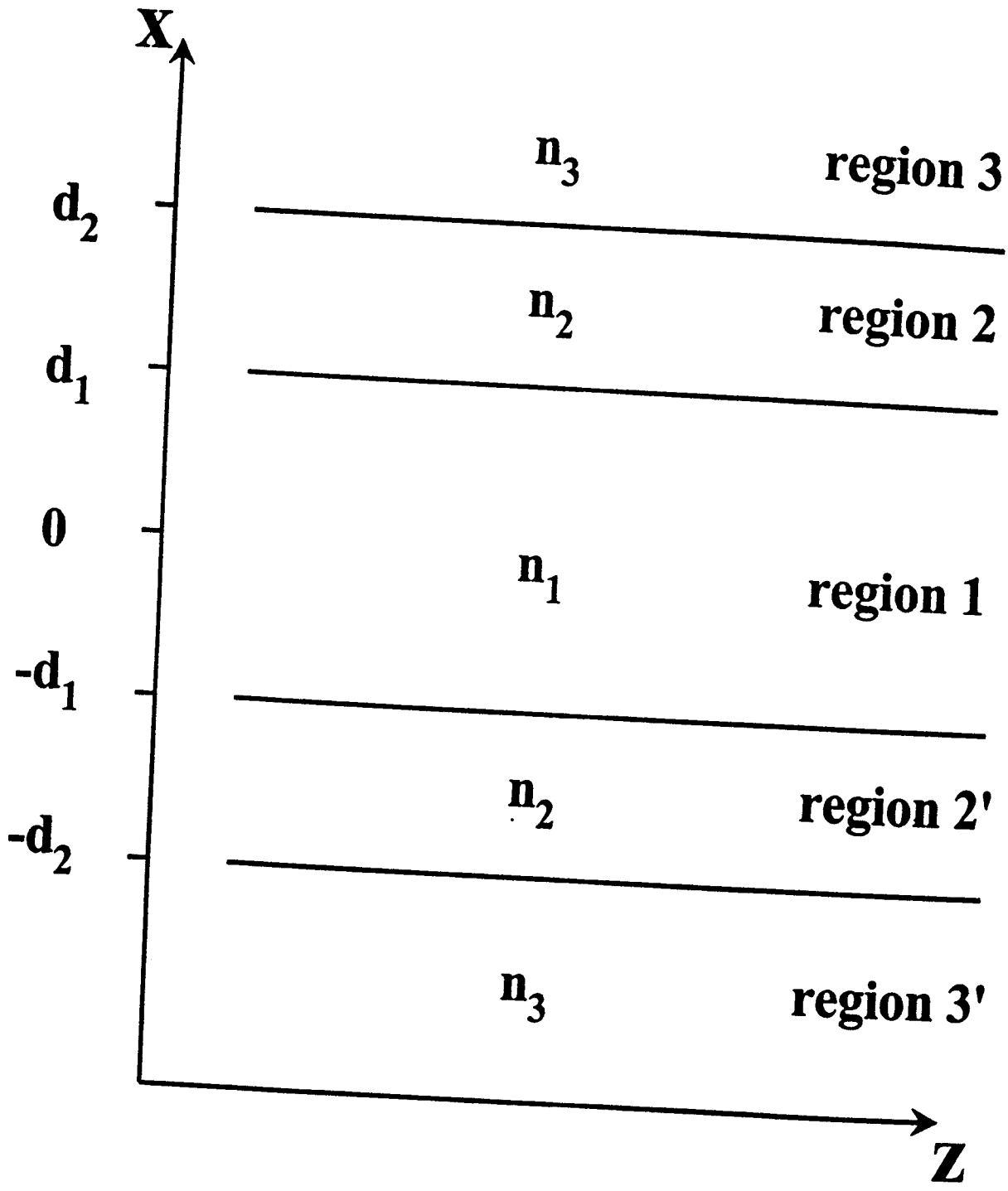
$n_3 < n_2 < n_1$
X
n_3
region 3
d_2
n_2
region 2
d_1
0
n_1
region 1
$-d_1$
n_2
region 2'
$-d_2$
n_3
region 3'
Z